

Geometrical Bioelectrodynamics

Vladimir G. Ivancevic and Tijana T. Ivancevic

Abstract

This paper proposes rigorous geometrical treatment of *bioelectrodynamics*, underpinning two fast-growing biomedical research fields: *bioelectromagnetism*, which deals with the ability of life to produce its own electromagnetism, and *bioelectromagnetics*, which deals with the effect on life from external electromagnetism.

Keywords: Bioelectrodynamics, exterior geometrical machinery, Dirac–Feynman quantum electrodynamics, functional electrical stimulation

Contents

1	Introduction	2
2	Exterior Geometrical Machinery in 4D	8
2.1	From Green to Stokes	8
2.2	Exterior derivative	9
2.3	Exterior p -forms in \mathbb{R}^4	9
2.4	Stokes Theorem in \mathbb{R}^4	13
2.5	Exact and closed p -forms and p -chains	13
2.6	Topological duality of p -forms and p -chains	14
2.7	The de Rham cochain complex	15
2.8	(Co)homology on a smooth manifold M	15
2.9	A cochain complex spanning the space-time manifold	16
2.10	Hodge star, codifferential and Laplacian	17
3	Classical Gauge Electrodynamics in 4D	18
3.1	Maxwell’s equations	19
3.2	Electrodynamic action	21
3.3	2D electrodynamics	22

4	Quantum Electrodynamics in 4D	22
4.1	Dirac QED	22
4.2	Feynman QED	25
4.3	Cohomology criterion for path–integral convergence	27
5	Electro–Muscular Stimulation	28
5.1	Global macro <i>EMS</i> –level	30
5.2	Local Micro <i>EMS</i> –level	32
5.3	Micro–Level Adaptation and Muscular Training	33
6	Appendix: Manifolds and Bundles	34
6.1	Manifolds	34
6.2	Fibre Bundles	35

1 Introduction

Bioelectromagnetism, sometimes equated with *bioelectricity*, bioelectromagnetism refers to the electrical, magnetic or electromagnetic fields produced by living cells, tissues or organisms. Examples include the cell potential of cell membranes and the electric currents that flow in nerves and muscles, as a result of action potentials. It is studied primarily through the techniques of *electrophysiology* (see, e.g. [1]), which is the study of the electrical properties of biological cells and tissues. It involves measurements of voltage change or electrical current flow on a wide variety of scales from single ion channel proteins to whole tissues like the heart. In neuroscience, it includes measurements of the electrical activity of neurons, and particularly *neural action potentials*, or neural spikes, pioneered by five celebrated Hodgkin-Huxley papers in 1952 [2, 3, 4, 5, 6] (formalized in [6] by a 1963-Nobel-Prize winning mathematical model), which are pulse-like waves of voltage that travel along several types of cell membranes. The best-understood example is generated on the membrane of the axon of a neuron, but also appears in other types of excitable cells, such as cardiac muscle cells, and even plant cells.¹ The principal ions

¹The resting voltage across the axonal membrane is typically -70 millivolts (mV), with the inside being more negative than the outside. As an action potential passes through a point, this voltage rises to roughly +40 mV in one millisecond, then returns to -70 mV. The action potential moves rapidly down the axon, with a conduction velocity as high as 100 meters/second (224 miles per hour). Because they are able to transmit information so fast, the flow of action potentials is a very efficient form of data transmission, considering that each neuron the signal passes through can be up to a meter in length. An action potential is provoked on a patch of membrane when the membrane is depolarized sufficiently, i.e., when the voltage of the cell’s interior relative to the cell’s exterior is raised above a threshold. Such a depolarization opens voltage-sensitive channels, which allows current to flow into the axon, further depolarizing the membrane. This will cause the membrane to ‘fire’, initiating a positive feedback loop that suddenly and rapidly causes the voltage inside the axon to become more positive. After this rapid rise, the membrane voltage is restored

involved in an action potential are sodium and potassium cations; sodium ions enter the cell, and potassium ions leave, restoring equilibrium. Relatively few ions need to cross the membrane for the membrane voltage to change drastically. The ions exchanged during an action potential, therefore, make a negligible change in the interior and exterior ionic concentrations. The few ions that do cross are pumped out again by the continual action of the sodium-potassium pump, which, with other ion transporters, maintains the normal ratio of ion concentrations across the membrane.² Calcium cations and chloride anions are involved in a few types of action potentials, such as the *cardiac action potential*³ [9].

to its resting value by a combination of effects: the channels responsible for the initial inward current are inactivated, while the raised voltage opens other voltage-sensitive channels that allow a compensating outward current. Because of the positive feedback, an action potential is all-or-none; there are no partial action potentials. In neurons, a typical action potential lasts for just a few thousandths of a second at any given point along their length. The passage of an action potential can leave the ion channels in a non-equilibrium state, making them more difficult to open, and thus inhibiting another action potential at the same spot: such an axon is said to be refractory.

²The action potential ‘travels’ along the axon without fading out because the signal is regenerated at each patch of membrane. This happens because an action potential at one patch raises the voltage at nearby patches, depolarizing them and provoking a new action potential there. In unmyelinated neurons, the patches are adjacent, but in myelinated neurons, the action potential ‘hops’ between distant patches, making the process both faster and more efficient. The axons of neurons generally branch, and an action potential often travels along both forks from a branch point. The action potential stops at the end of these branches, but usually causes the secretion of neurotransmitters at the synapses that are found there. These neurotransmitters bind to receptors on adjacent cells. These receptors are themselves ion channels, although in contrast to the axonal channels they are generally opened by the presence of a neurotransmitter, rather than by changes in voltage. The opening of these receptor channels can help to depolarize the membrane of the new cell (an excitatory channel) or work against its depolarization (an inhibitory channel). If these depolarizations are sufficiently strong, they can provoke another action potential in the new cell.

The flow of currents within an axon can be described quantitatively by *cable theory* [7] (as demonstrated by Hodgkin [8]). In simple cable theory, the neuron is treated as an electrically passive, perfectly cylindrical transmission cable, which can be described by a PDE:

$$\tau \frac{\partial V}{\partial t} = \lambda^2 \frac{\partial^2 V}{\partial x^2} - V,$$

where $V(x, t)$ is the voltage across the membrane at a time t and a position x along the length of the neuron, and where λ and τ are the characteristic length and time scales on which those voltages decay in response to a stimulus.

³The cardiac action potential differs from the neuronal action potential by having an extended plateau, in which the membrane is held at a high voltage for a few hundred milliseconds prior to being repolarized by the potassium current as usual. This plateau is due to the action of slower calcium channels opening and holding the membrane voltage near their equilibrium potential even after the sodium channels have inactivated. The cardiac action potential plays an important role in coordinating the contraction of the heart. The cardiac cells of the sinoatrial node provide the pacemaker potential that synchronizes the heart. The action potentials of those cells propagate to and through the atrioventricular node (AV node), which is normally the only conduction pathway between the atria and the ventricles. Action potentials from the AV node travel through the bundle of His and thence to the Purkinje fibers. Conversely, anomalies in the cardiac action potential, whether due to a congenital mutation or injury, can lead to human pathologies,

The action potential in a normal skeletal muscle cell is similar to the action potential in neurons [27, 22]. Action potentials result from the depolarization of the cell membrane (the sarcolemma), which opens voltage-sensitive sodium channels; these becomes inactivated and the membrane is repolarized through the outward current of potassium ions. The resting potential prior to the action potential is typically -90mV , somewhat more negative than typical neurons. The muscle action potential lasts roughly 24 ms, the absolute refractory period is roughly 13 ms, and the conduction velocity along the muscle is roughly 5 m/s. The action potential releases calcium ions that free up the tropomyosin and allow the muscle to contract. Muscle action potentials are provoked by the arrival of a pre-synaptic neuronal action potential at the neuromuscular junction. Their output is muscle force generation.

Bioelectromagnetic activity of the brain is measured by non-invasive *electroencephalography* (EEG), usually recorded from electrodes placed on the scalp⁴ (see, e.g. [11]). Normal brain wave patterns are classified by the frequency range as: delta ($< 4\text{Hz}$),⁵ theta ($4 - 7\text{Hz}$),⁶ alpha ($7 - 12\text{Hz}$),⁷ beta ($12 - 30\text{Hz}$),⁸ and gamma ($30 > \text{Hz}$).⁹

Bioelectromagnetic activity of the heart is measured by non-invasive *electrocardiography* especially arrhythmias (see, e.g. [10]).

⁴The data measured by the scalp EEG are used for clinical and research purposes. A technique similar to the EEG is intracranial EEG (icEEG), also referred to as subdural EEG (sdEEG) and electrocorticography (ECoG). These terms refer to the recording of activity from the surface of the brain (rather than the scalp). Because of the filtering characteristics of the skull and scalp, icEEG activity has a much higher spatial resolution than surface EEG.

⁵Delta is the highest in amplitude and the slowest in frequency. It is seen normally in adults in slow wave sleep. It is also seen normally in babies. It may occur focally with subcortical lesions and in general distribution with diffuse lesions, metabolic encephalopathy hydrocephalus or deep midline lesions. It is usually most prominent frontally in adults (e.g. Frontal Intermittent Rhythmic Delta) and posteriorly in children e.g. Occipital Intermittent Rhythmic Delta).

⁶Theta is seen normally in young children. It may be seen in drowsiness or arousal in older children and adults, as well as in meditation.

⁷Alpha is seen in the posterior regions of the head on both sides, being higher in amplitude on the dominant side. It is brought out by closing the eyes and by relaxation. It was noted to attenuate with eye opening or mental exertion. This activity is now referred to as ‘posterior basic rhythm’, the ‘posterior dominant rhythm’ or the ‘posterior alpha rhythm’, and is actually slower than 8Hz in young children (therefore technically in the theta range). In addition, there are two other normal alpha rhythms that are typically discussed: the Mu rhythm (which is an alpha-range activity that is seen over the sensorimotor cortex and characteristically attenuates with movement of the contralateral arm) and a temporal ‘third rhythm’.

⁸Beta is usually seen on both sides of the scalp in symmetrical distribution and is most evident frontally. Low amplitude beta with multiple and varying frequencies is often associated with active, busy or anxious thinking and active concentration.

⁹Because of the filtering properties of the skull and scalp, gamma rhythms can only be recorded from electrocorticography or possibly with magnetoencephalography. Gamma rhythms are thought to represent binding of different populations of neurons together into a network for the purpose of carrying out a certain cognitive or motor function.

raphy (ECG or EKG), usually recorded from electrodes placed on the skin of a thorax (see, e.g. [12]).¹⁰ Human heartbeats originate from the sinoatrial node (SA node) near the right atrium of the heart. Modified muscle cells contract, sending a signal to other muscle cells in the heart to contract. The signal spreads to the atrioventricular node (AV node). Signals carried from the AV node, slightly delayed, through bundle of His fibers and Purkinje fibers cause the ventricles to contract simultaneously. ECG measures changes in electrical potential across the heart, and can detect the contraction pulses that pass over the surface of the heart. There are three slow, negative changes, known as P, R, and T. Positive deflections are the Q and S waves. The P wave represents the contraction impulse of the atria, the T wave the ventricular contraction.¹¹

¹⁰Electrodes on different sides of the heart measure the activity of different parts of the heart muscle. An ECG displays the voltage between pairs of these electrodes, and the muscle activity that they measure, from different directions, also understood as vectors. This display indicates the overall rhythm of the heart, and weaknesses in different parts of the heart muscle. It is the best way to measure and diagnose abnormal rhythms of the heart, particularly abnormal rhythms caused by damage to the conductive tissue that carries electrical signals, or abnormal rhythms caused by levels of dissolved salts (electrolytes), such as potassium, that are too high or low. In myocardial infarction (MI), the ECG can identify damaged heart muscle. But it can only identify damage to muscle in certain areas, so it can't rule out damage in other areas. The ECG cannot reliably measure the pumping ability of the heart; for which ultrasound-based (echocardiography) or nuclear medicine tests are used.

¹¹The baseline voltage of the electrocardiogram is known as the *isoelectric line*. A typical ECG tracing of a normal heartbeat (or, cardiac cycle) consists of a P wave, a QRS complex and a T wave (see, e.g. [13]). A small U wave is normally visible in 50 to 75% of ECGs. During normal atrial depolarization, the mean electrical vector is directed from the SA node towards the AV node, and spreads from the right atrium to the left atrium. This turns into the P wave on the EKG, which is upright in II, III, and aVF (since the general electrical activity is going toward the positive electrode in those leads), and inverted in aVR (since it is going away from the positive electrode for that lead). The relationship between P waves and QRS complexes helps distinguish various cardiac arrhythmias. The shape and duration of the P waves may indicate atrial enlargement. The PR interval is measured from the beginning of the P wave to the beginning of the QRS complex. It is usually 0.12 to 0.20 s (120 to 200 ms). A prolonged PR interval may indicate a first degree heart block. A short PR interval may indicate an accessory pathway that leads to early activation of the ventricles, such as seen in Wolff–Parkinson–White syndrome. A variable PR interval may indicate other types of heart block. PR segment depression may indicate atrial injury or pericarditis. The QRS complex is a structure on the ECG that corresponds to the depolarization of the ventricles. Because the ventricles contain more muscle mass than the atria, the QRS complex is larger than the P wave. In addition, because the His/Purkinje system coordinates the depolarization of the ventricles, the QRS complex tends to look ‘spiked’ rather than rounded due to the increase in conduction velocity. A normal QRS complex is 0.06 to 0.10 sec (60 to 100 ms) in duration. Not every QRS complex contains a Q wave, an R wave, and an S wave. By convention, any combination of these waves can be referred to as a QRS complex. The duration, amplitude, and morphology of the QRS complex is useful in diagnosing cardiac arrhythmias, conduction abnormalities, ventricular hypertrophy, myocardial infarction, electrolyte derangements, and other disease states. Q waves can be normal (physiological) or pathological. The ST segment connects the QRS complex and the T wave and has a duration of 0.08 to 0.12 s (80 to 120 ms). It starts at the J point (junction between the QRS complex and ST segment) and ends at the beginning of the T wave. However, since it is usually difficult to determine exactly where the ST segment ends and the T wave begins, the relationship between the ST segment and T wave should be examined together. The

Bioelectromagnetic activity of skeletal muscles is measured by non-invasive *electromyography* (EMG), usually recorded from surface electrodes placed on the skin above working muscles.¹² An electromyograph detects the electrical potential generated by muscle cells, both when they contract or are at rest.¹³ A surface electrode may be used to monitor the general picture of muscle activation (see, e.g. [14]), as opposed to the activity of only a few fibres as observed using a needle. This technique is used in a number of settings; for example, in the physiotherapy clinic, muscle activation is monitored using surface EMG and patients have an auditory or visual stimulus to help them know when they are activating the muscle (biofeedback).¹⁴ EMG signals are essentially made up of superimposed motor unit action potentials (MUAPs) from several motor units. For a thorough analysis, the measured EMG signals can be decomposed into their constituent MUAPs. MUAPs from different motor units tend to have different characteristic shapes, while MUAPs recorded by the same electrode from the same motor unit are typically similar.¹⁵

Bioelectromagnetism should not to be confused with the similar word *bioelectromagnetics*, which deals with the effect on life from external electromagnetism (see, e.g. [16]). Supported by the Bioelectromagnetics Society (with Dr. Stefan Engström as President) and the scientific journal with the same name, bioelectromagnetics is the study of how electromagnetic fields interact with and influence biological processes. Common areas of investigation include the mechanism of animal migration and navigation using the ge-

typical ST segment duration is usually around 0.08 s (80 ms). It should be essentially level with the PR and TP segment. The normal ST segment has a slight upward concavity. Flat, down-sloping, or depressed ST segments may indicate coronary ischemia. ST segment elevation may indicate myocardial infarction.

¹²In contrast, to perform invasive intramuscular EMG, a needle electrode is inserted through the skin into the muscle tissue. The insertional activity provides valuable information about the state of the muscle and its innervating nerve.

¹³The electrical source is the muscle membrane potential of about -70mV. Measured EMG potentials range between less than 50 V and up to 20 to 30 mV, depending on the muscle under observation. Typical repetition rate of muscle unit firing is about 720 Hz, depending on the size of the muscle (eye muscles versus seat (gluteal) muscles), previous axonal damage and other factors. Damage to motor units can be expected at ranges between 450 and 780 mV.

¹⁴A motor unit is defined as one motor neuron and all of the muscle fibers it innervates. When a motor unit fires, the impulse (called an action potential) is carried down the motor neuron to the muscle. The area where the nerve contacts the muscle is called the neuromuscular junction, or the motor end plate. After the action potential is transmitted across the neuromuscular junction, an action potential is elicited in all of the innervated muscle fibers of that particular motor unit. The sum of all this electrical activity is known as a motor unit action potential (MUAP). This electrophysiologic activity from multiple motor units is the signal typically evaluated during an EMG. The composition of the motor unit, the number of muscle fibres per motor unit, the metabolic type of muscle fibres and many other factors affect the shape of the motor unit potentials in the myogram. Nerve conduction testing is also often done at the same time as an EMG in order to diagnose neurological diseases.

¹⁵Notably MUAP size and shape depend on where the electrode is located with respect to the fibers and so can appear to be different if the electrode moves position. EMG decomposition is non-trivial, although many methods have been proposed (see, e.g. [15]).

omagnetic field, studying the potential effects of man-made sources of electromagnetic fields, such as those produced by the power distribution system and mobile phones, and developing novel therapies to treat various conditions.

Most importantly, in recent years a growing number of people have begun to use mobile phone technology. This phenomenon has raised questions and doubts about possible effects on users' brains. The recent literature review presented in [17] has focused on the human electrophysiological and neuro-metabolic effects of mobile phone (MP)- related electromagnetic fields (EMFs) published in the last 10 years. All relevant papers have been reported and, subsequently, a literature selection has been carried out by taking several criteria into account, such as: blind techniques, randomization or counter-balancing of conditions and subjects, detail of exposure characteristics and the statistical analyses used. As a result, only the studies meeting the selection criteria have been described, evaluated and discussed further. This review has provided a clear scenario of the most reliable experiments carried out over the last decade and to offer a critical point of view in their evaluation. Its conclusion is that MP-EMFs may influence normal physiology through changes in cortical excitability and that in future research particular care should be dedicated to both methodological and statistical control, the most relevant criteria in this research field.

More generally, epidemiological studies of radio frequency (RF) exposures and human cancers include studies of military and civilian occupational groups, people who live near television and radio transmitters, and users of mobile phones. Many types of cancer have been assessed in [18], with particular attention given to leukemia and brain tumors. The presented epidemiological results fall short of the strength and consistency of evidence that is required to come to a conclusion that RF emissions are a cause of human cancer. Although the epidemiological evidence in total suggests no increased risk of cancer, the results cannot be unequivocally interpreted in terms of cause and effect. The results are inconsistent, and most studies are limited by lack of detail on actual exposures, short follow-up periods, and the limited ability to deal with other relevant factors. For these reasons, the studies are unable to confidently exclude any possibility of an increased risk of cancer. Further research to clarify the situation is justified. Priorities include further studies of leukemia in both adults and children, and of cranial tumors in relationship to mobile phone use.

In a recent technical paper [19], a new theoretical treatment of ion resonance phenomena was formulated around the *Lorentz force equation*. This equation defines the motion of a particle of mass m and charge q moving with a mean time τ in a joint electric field \mathbf{E} and magnetic field \mathbf{B}

$$m\dot{\mathbf{v}} + m\mathbf{v}/\tau = q(\mathbf{E} + \mathbf{v} \times \mathbf{B}), \quad (1)$$

where overdot means time derivative and \times is the vector cross-product. The authors derive an expression for the velocity of a damped ion with arbitrary q/m under the influence

of the Lorentz force on the right-hand side of (1). Series solutions to the differential equations reveal transient responses as well as resonance-like terms. An important result in this field is that the expressions for ionic drift velocity include a somewhat similar Bessel function dependence as was previously obtained for the transition probability in parametric resonance. The authors have found an explicit effect due to damping, so that previous Bessel dependence now occurs as a subset of a more general solution, including not only the magnetic field AC/DC ratio as an independent variable, but also the ratio of the cyclotronic frequency Ω to the applied AC frequency ω . The authors hypothesize that the selectively enhanced drift velocity predicted in their model can explain ICR-like phenomena as resulting from increased interaction probabilities in the vicinity of ion channel gates.

This paper proposes rigorous geometrical *bioelectrodynamics*, which we define to be the common field theory underpinning both bioelectromagnetism and bioelectromagnetics.

2 Exterior Geometrical Machinery in 4D

2.1 From Green to Stokes

Recall that *Green's Theorem* in the region C in (x, y) -plane \mathbb{R}^2 connects a line integral $\oint_{\partial C}$ (over the boundary ∂C of C) with a double integral \iint_C over C (see e.g., [20])

$$\oint_{\partial C} Pdx + Qdy = \iint_C \left(\frac{\partial Q}{\partial x} - \frac{\partial P}{\partial y} \right) dxdy.$$

In other words, if we define two differential forms (integrands of $\oint_{\partial C}$ and \iint_C) as

$$\begin{aligned} \text{1-form} & : \mathbf{A} = Pdx + Qdy, & \text{and} \\ \text{2-form} & : \mathbf{dA} = \left(\frac{\partial Q}{\partial x} - \frac{\partial P}{\partial y} \right) dxdy, \end{aligned}$$

(where \mathbf{d} denotes the *exterior derivative* that makes a $(p+1)$ -form out of a p -form, see next subsection), then we can rewrite Green's theorem as *Stokes' theorem*:

$$\int_{\partial C} \mathbf{A} = \int_C \mathbf{dA}.$$

The integration domain C is in topology called a *chain*, and ∂C is a 1D boundary of a 2D chain C . In general, *the boundary of a boundary is zero* (see [35, 36]), that is, $\partial(\partial C) = 0$, or formally $\partial^2 = 0$.

2.2 Exterior derivative

The exterior derivative \mathbf{d} is a generalization of ordinary vector differential operators (*grad*, *div* and *curl* see e.g., [34]) that transforms p -forms ω into $(p+1)$ -forms $\mathbf{d}\omega$ (see next subsection), with the main property: $\mathbf{d}\mathbf{d} = \mathbf{d}^2 = 0$, so that in \mathbb{R}^3 we have (see Figures 1 and 2)

- any scalar function $f = f(x, y, z)$ is a 0-form;
- the gradient $\mathbf{d}f = \omega$ of any smooth function f is a 1-form

$$\omega = \mathbf{d}f = \frac{\partial f}{\partial x}dx + \frac{\partial f}{\partial y}dy + \frac{\partial f}{\partial z}dz;$$

- the curl $\alpha = \mathbf{d}\omega$ of any smooth 1-form ω is a 2-form

$$\alpha = \mathbf{d}\omega = \left(\frac{\partial R}{\partial y} - \frac{\partial Q}{\partial z} \right) dydz + \left(\frac{\partial P}{\partial z} - \frac{\partial R}{\partial x} \right) dzdx + \left(\frac{\partial Q}{\partial x} - \frac{\partial P}{\partial y} \right) dxdy;$$

if $\omega = \mathbf{d}f \Rightarrow \alpha = \mathbf{d}\mathbf{d}f = 0$.

- the divergence $\beta = \mathbf{d}\alpha$ of any smooth 2-form α is a 3-form

$$\beta = \mathbf{d}\alpha = \left(\frac{\partial A}{\partial x} + \frac{\partial B}{\partial y} + \frac{\partial C}{\partial z} \right) dxdydz; \quad \text{if } \alpha = \mathbf{d}\omega \Rightarrow \beta = \mathbf{d}\mathbf{d}\omega = 0.$$

In general, for any two smooth functions $f = f(x, y, z)$ and $g = g(x, y, z)$, the exterior derivative \mathbf{d} obeys the *Leibniz rule* [23, 24]:

$$\mathbf{d}(fg) = g \mathbf{d}f + f \mathbf{d}g,$$

and the *chain rule*:

$$\mathbf{d}(g(f)) = g'(f) \mathbf{d}f.$$

2.3 Exterior p -forms in \mathbb{R}^4

In general, given a so-called 4D *coframe*, that is a set of coordinate differentials $\{dx^i\} \in \mathbb{R}^4$, we can define the space of all p -forms, denoted $\Omega^p(\mathbb{R}^4)$, using the exterior derivative $\mathbf{d} : \Omega^p(\mathbb{R}^4) \rightarrow \Omega^{p+1}(\mathbb{R}^4)$ and Einstein's summation convention over repeated indices (e.g., $A_i dx^i = \sum_{i=0}^3 A_i dx^i$), we have:

1-form – a generalization of the Green's 1-form $Pdx + Qdy$,

$$\mathbf{A} = A_i dx^i \in \Omega^1(\mathbb{R}^4).$$

For example, in 4D electrodynamics, \mathbf{A} represents electromagnetic (co)vector potential.

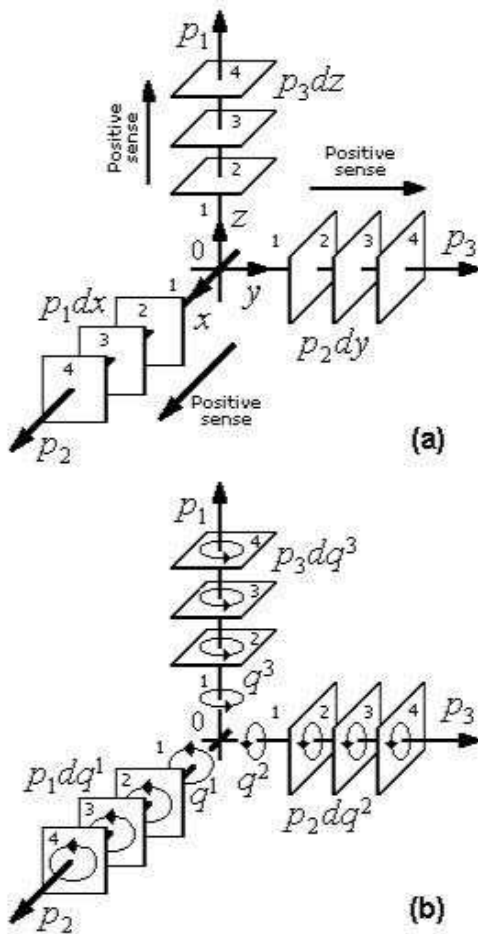


Figure 1: Basis vectors and one-forms in Euclidean \mathbb{R}^3 -space: (a) Translational case; and (b) Rotational case [21]. For the same geometry in \mathbb{R}^3 , see [35].

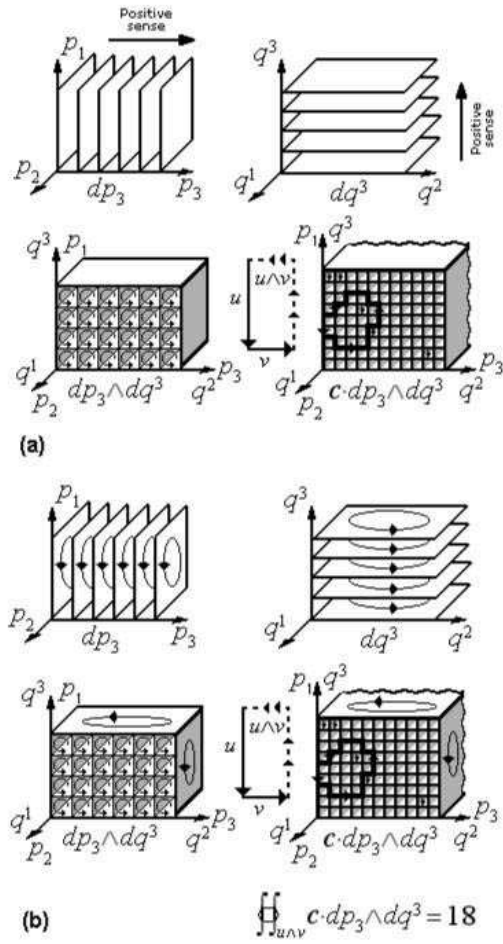


Figure 2: Fundamental two-form and its flux in \mathbb{R}^3 : (a) Translational case; (b) Rotational case. In both cases the flux through the plane $u \wedge v$ is defined as $\int \int_{u \wedge v} c dp_i dq^i$ and measured by the number of tubes crossed by the circulation oriented by $u \wedge v$ [21]. For the same geometry in \mathbb{R}^3 , see [35].

2-form – generalizing the Green’s 2-form $(\partial_x Q - \partial_y P) dx dy$ (with $\partial_j = \partial/\partial x^j$),

$$\begin{aligned} \mathbf{B} &= \mathbf{dA} \in \Omega^2(\mathbb{R}^4), & \text{with components} \\ \mathbf{B} &= \frac{1}{2} B_{ij} dx^i \wedge dx^j, & \text{or} \\ \mathbf{B} &= \partial_j A_i dx^j \wedge dx^i, & \text{so that} \\ B_{ij} &= -2\partial_j A_i = \partial_i A_j - \partial_j A_i = -B_{ji}. \end{aligned}$$

where \wedge is the anticommutative exterior (or, ‘wedge’) product of two differential forms; given a p -form $\alpha \in \Omega^p(\mathbb{R}^4)$ and a q -form $\beta \in \Omega^q(\mathbb{R}^4)$, their exterior product is a $(p+q)$ -form $\alpha \wedge \beta \in \Omega^{p+q}(\mathbb{R}^4)$; e.g., if we have two 1-forms $\mathbf{a} = a_i dx^i$, and $\mathbf{b} = b_i dx^i$, their wedge product $\mathbf{a} \wedge \mathbf{b}$ is a 2-form α given by

$$\alpha = \mathbf{a} \wedge \mathbf{b} = a_i b_j dx^i \wedge dx^j = -a_i b_j dx^j \wedge dx^i = -\mathbf{b} \wedge \mathbf{a}.$$

The exterior product \wedge is related to the exterior derivative \mathbf{d} , by

$$\mathbf{d}(\alpha \wedge \beta) = \mathbf{d}\alpha \wedge \beta + (-1)^p \alpha \wedge \mathbf{d}\beta.$$

3-form

$$\begin{aligned} \mathbf{C} &= \mathbf{dB} (= \mathbf{d}\mathbf{dA} \equiv 0) \in \Omega^3(\mathbb{R}^4), & \text{with components} \\ \mathbf{C} &= \frac{1}{3!} C_{ijk} dx^i \wedge dx^j \wedge dx^k, & \text{or} \\ \mathbf{C} &= \partial_k B_{[ij]} dx^k \wedge dx^i \wedge dx^j, & \text{so that} \\ C_{ijk} &= -6\partial_k B_{[ij]}, & \text{where } B_{[ij]} \text{ is the skew-symmetric part of } B_{ij}. \end{aligned}$$

For example, in the 4D electrodynamics, \mathbf{B} represents the field 2-form *Faraday*, or the Liénard–Wiechert 2-form (in the next section we will use the standard symbol \mathbf{F} instead of \mathbf{B}) satisfying the sourceless magnetic Maxwell’s equation,

$$\text{Bianchi identity : } \mathbf{d}\mathbf{B} = 0, \quad \text{in components } \partial_k B_{[ij]} = 0.$$

4-form

$$\begin{aligned} \mathbf{D} &= \mathbf{dC} (= \mathbf{d}\mathbf{dB} \equiv 0) \in \Omega^4(\mathbb{R}^4), & \text{with components} \\ \mathbf{D} &= \partial_l C_{[ijk]} dx^l \wedge dx^i \wedge dx^j \wedge dx^k, & \text{or} \\ \mathbf{D} &= \frac{1}{4!} D_{ijkl} dx^i \wedge dx^j \wedge dx^k \wedge dx^l, & \text{so that} \\ D_{ijkl} &= -24\partial_l C_{[ijk]}. \end{aligned}$$

2.4 Stokes Theorem in \mathbb{R}^4

Generalization of the Green's theorem in the plane (and all other integral theorems from vector calculus) is the Stokes Theorem for the p -form ω , in the n D domain C (which is a p -chain with a $(p - 1)$ -boundary ∂C , see next subsection)

$$\int_{\partial C} \omega = \int_C \mathbf{d}\omega.$$

In the 4D Euclidean space \mathbb{R}^4 we have the following three particular cases of the Stokes theorem, related to the subspaces C of \mathbb{R}^4 :

The 2D Stokes theorem:

$$\int_{\partial C^2} \mathbf{A} = \int_{C^2} \mathbf{B}.$$

The 3D Stokes theorem:

$$\int_{\partial C^3} \mathbf{B} = \int_{C^3} \mathbf{C}.$$

The 4D Stokes theorem:

$$\int_{\partial C^4} \mathbf{C} = \int_{C^4} \mathbf{D}.$$

2.5 Exact and closed p -forms and p -chains

Notation: we drop boldface letters from now on. In general, a p -form β is called *closed* if its exterior derivative is equal to zero,

$$d\beta = 0.$$

From this condition one can see that the closed form (the *kernel* of the exterior derivative operator d) is conserved quantity. Therefore, closed p -forms possess certain invariant properties, physically corresponding to the conservation laws (see e.g., [30]).

Also, a p -form β that is an exterior derivative of some $(p - 1)$ -form α ,

$$\beta = d\alpha,$$

is called *exact* (the *image* of the exterior derivative operator d). By Poincaré Lemma, exact forms prove to be closed automatically,

$$d\beta = d(d\alpha) = 0.$$

Since $d^2 = 0$, *every exact form is closed*. The converse is only partially true (Poincaré Lemma): every closed form is *locally exact*. This means that given a closed p -form on a smooth manifold M (see Appendix), $\alpha \in \Omega^p(M)$ on an open set $U \subset M$, any point $m \in U$ has a neighborhood on which there exists a $(p-1)$ -form $\beta \in \Omega^{p-1}(U)$ such that $d\beta = \alpha|_U$.

The Poincaré lemma is a generalization and unification of two well-known facts in vector calculus:

(i) If $\text{curl } F = 0$, then locally $F = \text{grad } f$; and (ii) If $\text{div } F = 0$, then locally $F = \text{curl } G$.

Poincaré lemma for contractible manifolds: Any closed form on a smoothly contractible manifold is exact.

A *cycle* is a chain $C \in \mathcal{C}_p(M)$ such that $\partial C = 0$. A *boundary* is a chain C such that $C = \partial B$, for any other chain $B \in \mathcal{C}_p(M)$. Similarly, a *cocycle* (i.e., a *closed form*) is a cochain ω such that $d\omega = 0$. A *coboundary* (i.e., an *exact form*) is a cochain ω such that $\omega = d\theta$, for any other cochain θ . All exact forms are closed ($\omega = d\theta \Rightarrow d\omega = 0$) and all boundaries are cycles ($C = \partial B \Rightarrow \partial C = 0$). Converse is true only for smooth contractible manifolds, by Poincaré Lemma.

2.6 Topological duality of p -forms and p -chains

Duality of p -forms and p -chains on a smooth manifold M is based on the

$$\text{Period: } \int_C \omega := \langle C, \omega \rangle,$$

where C is a cycle, ω is a cocycle, while $\langle C, \omega \rangle = \omega(C)$ is their inner product $\langle C, \omega \rangle : \Omega^p(M) \times \mathcal{C}_p(M) \rightarrow \mathbb{R}$, a bilinear non-degenerate functional (pairing) on M [31]. From Poincaré Lemma, a closed p -form ω is exact iff $\langle C, \omega \rangle = 0$.

The fundamental topological duality is based on the Stokes theorem,

$$\int_{\partial C} \omega = \int_C d\omega \quad \text{or} \quad \langle \partial C, \omega \rangle = \langle C, d\omega \rangle,$$

where ∂C is the boundary of the p -chain C oriented coherently with C on M . While the *boundary operator* ∂ is a global operator, the coboundary operator d is local, and thus more suitable for applications. The main property of the exterior differential,

$$d \circ d \equiv d^2 = 0 \quad \implies \quad \partial \circ \partial \equiv \partial^2 = 0, \quad (\text{and converse}),$$

can be easily proved using the Stokes' theorem as

$$0 = \langle \partial^2 C, \omega \rangle = \langle \partial C, d\omega \rangle = \langle C, d^2 \omega \rangle = 0.$$

2.7 The de Rham cochain complex

In the Euclidean 3D space \mathbb{R}^3 we have the following de Rham *cochain complex*

$$0 \rightarrow \Omega^0(\mathbb{R}^3) \xrightarrow[\text{grad}]{d} \Omega^1(\mathbb{R}^3) \xrightarrow[\text{curl}]{d} \Omega^2(\mathbb{R}^3) \xrightarrow[\text{div}]{d} \Omega^3(\mathbb{R}^3) \rightarrow 0.$$

Using the *closure property* for the exterior differential in \mathbb{R}^3 , $d \circ d \equiv d^2 = 0$, we get the standard identities from vector calculus

$$\text{curl} \cdot \text{grad} = 0 \quad \text{and} \quad \text{div} \cdot \text{curl} = 0.$$

As a duality, in \mathbb{R}^3 we have the following *chain complex*

$$0 \leftarrow \mathcal{C}_0(\mathbb{R}^3) \xleftarrow{\partial} \mathcal{C}_1(\mathbb{R}^3) \xleftarrow{\partial} \mathcal{C}_2(\mathbb{R}^3) \xleftarrow{\partial} \mathcal{C}_3(\mathbb{R}^3) \leftarrow 0,$$

(with the closure property $\partial \circ \partial \equiv \partial^2 = 0$) which implies the following three boundaries:

$$C_1 \xrightarrow{\partial} C_0 = \partial(C_1), \quad C_2 \xrightarrow{\partial} C_1 = \partial(C_2), \quad C_3 \xrightarrow{\partial} C_2 = \partial(C_3),$$

where $C_0 \in \mathcal{C}_0$ is a 0–boundary (or, a point), $C_1 \in \mathcal{C}_1$ is a 1–boundary (or, a line), $C_2 \in \mathcal{C}_2$ is a 2–boundary (or, a surface), and $C_3 \in \mathcal{C}_3$ is a 3–boundary (or, a hypersurface). Similarly, the de Rham complex implies the following three coboundaries:

$$C^0 \xrightarrow{d} C^1 = d(C^0), \quad C^1 \xrightarrow{d} C^2 = d(C^1), \quad C^2 \xrightarrow{d} C^3 = d(C^2),$$

where $C^0 \in \Omega^0$ is 0–form (or, a function), $C^1 \in \Omega^1$ is a 1–form, $C^2 \in \Omega^2$ is a 2–form, and $C^3 \in \Omega^3$ is a 3–form.

In general, on a smooth n D manifold M we have the following de Rham cochain complex [33]

$$0 \rightarrow \Omega^0(M) \xrightarrow{d} \Omega^1(M) \xrightarrow{d} \Omega^2(M) \xrightarrow{d} \Omega^3(M) \xrightarrow{d} \dots \xrightarrow{d} \Omega^n(M) \rightarrow 0,$$

satisfying the closure property on M , $d \circ d \equiv d^2 = 0$.

2.8 (Co)homology on a smooth manifold M

The subspace of all closed p –forms (cocycles) on a smooth manifold M is the kernel $\text{Ker}(d)$ of the de Rham d –homomorphism (see Figure 3), denoted by $Z^p(M) \subset \Omega^p(M)$, and the sub-subspace of all exact p –forms (coboundaries) on M is the image $\text{Im}(d)$ of the de Rham homomorphism denoted by $B^p(M) \subset Z^p(M)$. The *quotient space*

$$H^p(M) := \frac{Z^p(M)}{B^p(M)} = \frac{\text{Ker}(d : \Omega^p(M) \rightarrow \Omega^{p+1}(M))}{\text{Im}(d : \Omega^{p-1}(M) \rightarrow \Omega^p(M))},$$

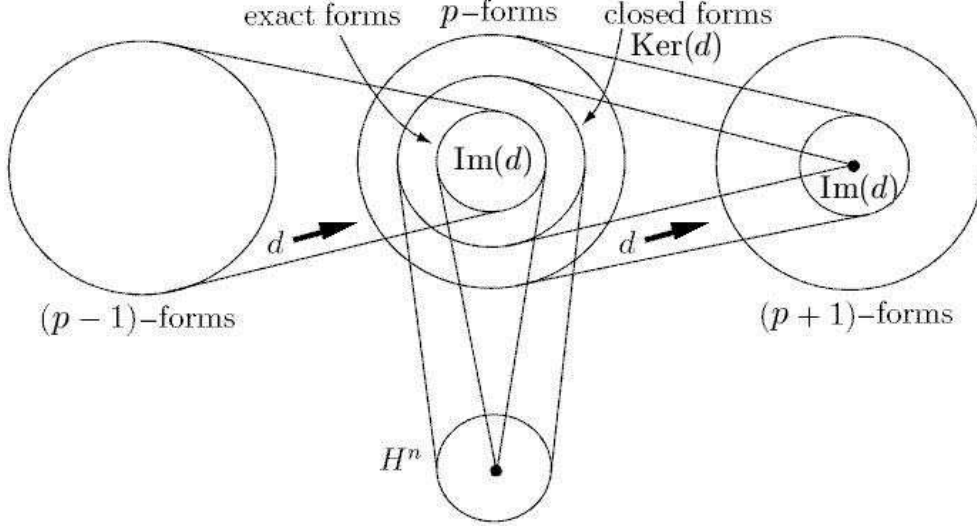


Figure 3: A small portion of the de Rham cochain complex, showing a homomorphism of cohomology groups.

is called the p th *cohomology group* of a manifold M . It is a topological invariant of a manifold. Two p -cocycles $\alpha, \beta \in \Omega^p(M)$ are *homologous*, or belong to the same *cohomology class* $[\alpha] \in H^p(M)$, if they differ by a $(p-1)$ -coboundary $\alpha - \beta = d\theta \in \Omega^{p-1}(M)$.

Similarly, the subspace of all p -cycles on a smooth manifold M is the kernel $\text{Ker}(\partial)$ of the ∂ -homomorphism, denoted by $Z_p(M) \subset \mathcal{C}_p(M)$, and the sub-subspace of all p -boundaries on M is the image $\text{Im}(\partial)$ of the ∂ -homomorphism, denoted by $B_p(M) \subset \mathcal{C}_p(M)$. Two p -cycles $C_1, C_2 \in \mathcal{C}_p$ are *homologous*, if they differ by a $(p-1)$ -boundary $C_1 - C_2 = \partial B \in \mathcal{C}_{p-1}(M)$. Then C_1 and C_2 belong to the same *homology class* $[C] \in H_p(M)$, which is defined as

$$H_p(M) := \frac{Z_p(M)}{B_p(M)} = \frac{\text{Ker}(\partial : \mathcal{C}_p(M) \rightarrow \mathcal{C}_{p-1}(M))}{\text{Im}(\partial : \mathcal{C}_{p+1}(M) \rightarrow \mathcal{C}_p(M))},$$

where Z_p is the vector space of cycles and $B_p \subset Z_p$ is the vector space of boundaries on M .

2.9 A cochain complex spanning the space-time manifold

Consider a small portion of the de Rham cochain complex of Figure 3 spanning a space-time 4-manifold M ,

$$\Omega^{p-1}(M) \xrightarrow{d_{p-1}} \Omega^p(M) \xrightarrow{d_p} \Omega^{p+1}(M)$$

As we have seen above, cohomology classifies topological spaces by comparing two subspaces of Ω^p : (i) the space of p -cocycles, $Z^p(M) := \text{Ker } d_p$, and (ii) the space of p -coboundaries, $B^p(M) := \text{Im } d_{p-1}$. Thus, for the cochain complex of any space-time 4-manifold we have,

$$d^2 = 0 \implies B^p(M) \subset Z^p(M),$$

that is, every p -coboundary is a p -cocycle. Whether the converse of this statement is true, according to Poincaré Lemma, depends on the particular topology of a space-time 4-manifold. If every p -cocycle is a p -coboundary, so that B^p and Z^p are equal, then the cochain complex is exact at $\Omega^p(M)$. In topologically interesting regions of a space-time manifold M , exactness may fail, and we measure the failure of exactness by taking the p th cohomology group

$$H^p(M) := Z^p(M)/B^p(M).$$

2.10 Hodge star, codifferential and Laplacian

The *Hodge star* operator $\star : \Omega^p(M) \rightarrow \Omega^{n-p}(M)$ on a smooth manifold M is defined as [32]

$$\alpha \wedge \star \beta = \beta \wedge \star \alpha = \langle \alpha, \beta \rangle \mu, \quad \text{for } \alpha, \beta \in \Omega^p(M).$$

The \star operator depends on the Riemannian metric on M and also on the orientation (reversing orientation will change the sign). The *volume form* μ is defined in local coordinates on M as

$$\mu = \text{vol} = \star(1) = \sqrt{\det(g_{ij})} dx^1 \wedge \dots \wedge dx^n,$$

and the total volume on M is given by

$$\text{vol}(M) = \int_M \star(1).$$

For example, in the 4D electrodynamics, the dual 2-form *Maxwell* $\star F$ satisfies the electric Maxwell equation with the source [35],

$$\text{Dual Bianchi identity : } \mathbf{d}\star\mathbf{F} = \star\mathbf{J},$$

where $\star\mathbf{J}$ is the 3-form dual to the charge-current 1-form \mathbf{J} .

For any two p -forms $\alpha, \beta \in \Omega^p(M)$ with compact support, we define the (bilinear and positive-definite) Hodge L^2 -inner product as

$$(\alpha, \beta) = \int_M \langle \alpha, \beta \rangle \star(1) = \int_M \alpha \wedge \star\beta. \quad (2)$$

We can extend the product (\cdot, \cdot) to $L^2(\Omega^p(M))$; it remains bilinear and positive-definite, because as usual in the definition of L^2 , functions that differ only on a set of measure zero are identified.

Now, the Hodge dual to the exterior derivative $d : \Omega^p(M) \rightarrow \Omega^{p+1}(M)$ on a smooth manifold M is the *codifferential* δ , a linear map $\delta : \Omega^p(M) \rightarrow \Omega^{p-1}(M)$, which is a generalization of the divergence, defined by [32]

$$\delta = \star d \star (-1)^{n(p+1)+1}, \quad \text{so that} \quad d = \star \delta \star (-1)^{np}.$$

Applied to any p -form $\omega \in \Omega^p(M)$, the codifferential δ gives

$$\delta\omega = (-1)^{n(p+1)+1} \star d \star \omega.$$

If $\omega = f$ is a 0-form, or function, then $\delta f = 0$.

The codifferential δ can be coupled with the exterior derivative d to construct the *Hodge Laplacian* $\Delta : \Omega^p(M) \rightarrow \Omega^p(M)$, a harmonic generalization of the Laplace–Beltrami differential operator, given by¹⁶

$$\Delta = \delta d + d\delta.$$

The Hodge codifferential δ satisfies the following set of rules:

- $\delta\delta = \delta^2 = 0$, the same as $dd = d^2 = 0$;
- $\delta\Delta = \Delta\delta$, the same as $d\Delta = \Delta d$;
- $\delta\star = (-1)^{p+1} \star d$; $\star\delta = (-1)^p \star d$;
- $d\delta\star = \star\delta d$; $\star d\delta = \delta d\star$; $\star\Delta = \Delta\star$.

3 Classical Gauge Electrodynamics in 4D

Recall that a *gauge theory* is a theory that admits a symmetry with a local parameter. For example, in every quantum theory the global phase of the wave ψ -function is arbitrary and does not represent something physical. Consequently, the theory is invariant under a global change of phases (adding a constant to the phase of all wave functions, everywhere); this is a global symmetry. In quantum electrodynamics, the theory is also invariant under a local change of phase, that is, one may shift the phase of all wave functions so that the shift may be different at every point in space-time. This is a local symmetry. However, in order for a well-defined derivative operator to exist, one must introduce a new field, the *gauge field*, which also transforms in order for the local change of variables (the phase in our example) not to affect the derivative. In quantum electrodynamics this gauge field is the electromagnetic potential 1-form A , in components given by

$$A = A_\mu dx^\mu, \quad \text{such that} \quad A_{\text{new}} = A_{\text{old}} + df,$$

¹⁶The difference $d - \delta = \partial_D$ is called the *Dirac operator*. Its square ∂_D^2 equals the Hodge Laplacian Δ .

(where f is an arbitrary scalar function) – leaves the electromagnetic field 2–form $F = dA$ unchanged. This change df of local gauge of variable A is termed *gauge transformation*. In quantum field theory the excitations of fields represent particles. The particle associated with excitations of the gauge field is the *gauge boson*. All the fundamental interactions in nature are described by gauge theories. In particular, in quantum electrodynamics, whose gauge transformation is a local change of phase, the gauge group is the circle group $U(1)$ (consisting of all complex numbers with absolute value 1), and the gauge boson is the photon (see e.g., [37]).

In the 4D space-time electrodynamics, the 1–form *electric current density* J has the components $J_\mu = (\rho, \mathbf{j}) = (\rho, j_x, j_y, j_z)$ (where ρ is the charge density), the 2–form *Faraday* F is given in components of electric field \mathbf{E} and magnetic field \mathbf{B} by

$$F_{\mu\nu} = \begin{pmatrix} 0 & E_x & E_y & E_z \\ -E_x & 0 & -B_z & B_y \\ -E_y & B_z & 0 & -B_x \\ -E_z & -B_y & B_x & 0 \end{pmatrix}, \quad \text{with} \quad F_{\nu\mu} = -F_{\mu\nu}$$

while its dual 2–form *Maxwell* $\star F$ has the following components

$$\star F_{\mu\nu} = \begin{pmatrix} 0 & -B_x & -B_y & -B_z \\ B_x & 0 & -E_z & E_y \\ B_y & E_z & 0 & -E_x \\ B_z & -E_y & B_x & 0 \end{pmatrix}, \quad \text{with} \quad \star F_{\nu\mu} = -\star F_{\mu\nu}.$$

3.1 Maxwell's equations

The *gauge field* in classical electrodynamics, in local coordinates given as an electromagnetic potential 1–form

$$A = A_\mu dx^\mu = A_\mu dx^\mu + df, \quad (f = \text{arbitrary scalar field}),$$

is globally a *connection* on a $U(1)$ -bundle¹⁷ (see Appendix). The corresponding electromagnetic field, locally the 2-form

$$\begin{aligned} F &= dA, & \text{in components given by} \\ F &= \frac{1}{2}F_{\mu\nu} dx^\mu \wedge dx^\nu, & \text{with } F_{\mu\nu} = \partial_\nu A_\mu - \partial_\mu A_\nu \end{aligned}$$

is globally the *curvature* of the connection A ¹⁸ under the gauge-covariant derivative,

$$D_\mu = \partial_\mu - ieA_\mu,$$

where $i = \sqrt{-1}$ and e is the charge coupling constant.¹⁹

¹⁷Recall that in the 19th Century, Maxwell unified Faraday's electric and magnetic fields. Maxwell's theory led to Einstein's special relativity where this unification becomes a spin-off of the unification of space and time in the form of the *Faraday tensor* [35]

$$F = E \wedge dt + B,$$

where F is electromagnetic 2-form on space-time, E is electric 1-form on space, and B is magnetic 2-form on space. Gauge theory considers F as secondary object to a connection-potential 1-form A . This makes half of the Maxwell equations into tautologies [38], i.e.,

$$F = dA \implies dF = 0 \quad : \quad \text{Bianchi identity,}$$

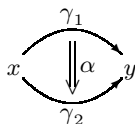
but does not imply the second half of Maxwell's equations,

$$\delta F = -4\pi J \quad : \quad \text{dual Bianchi identity.}$$

To understand the deeper meaning of the connection-potential 1-form A , we can integrate it along a path γ in space-time, $x \xrightarrow{\gamma} y$. Classically, the integral $\int_\gamma A$ represents an *action* for a charged point particle to move along the path γ . Quantum-mechanically, $\exp\left(i \int_\gamma A\right)$ represents a *phase* (within the unitary Lie group $U(1)$) by which the particle's wave-function changes as it moves along the path γ , so A is a $U(1)$ -connection.

In other words, Maxwell's equations can be formulated using complex line bundles, or principal bundles with fibre $U(1)$. The connection ∇ on the line bundle has a curvature $F = \nabla^2$ which is a 2-form that automatically satisfies $dF = 0$ and can be interpreted as a field-strength. If the line bundle is trivial with flat reference connection d , we can write $\nabla = d + A$ and $F = dA$ with A the 1-form composed of the electric potential and the magnetic vector potential.

¹⁸The only thing that matters here is the *difference* α between two paths γ_1 and γ_2 in the action $\int_\gamma A$ [38], which is a 2-morphism (see e.g., [23, 24])



¹⁹If a gauge transformation is given by

$$\psi \mapsto e^{i\Lambda} \psi$$

Classical electrodynamics is governed by the *Maxwell equations*, which in exterior formulation read

$$\begin{aligned} dF &= 0, & \delta F &= -4\pi J, & \text{or in components,} \\ F_{[\mu\nu,\eta]} &= 0, & F_{\mu\nu,\mu} &= -4\pi J_\mu, \end{aligned}$$

where comma denotes the partial derivative and the 1-form of electric current $J = J_\mu dx^\mu$ is conserved, by the electrical *continuity equation*,

$$\delta J = 0, \quad \text{or in components,} \quad J_{\mu,\mu} = 0.$$

The first, sourceless Maxwell equation, $dF = 0$, gives vector magnetostatics and magnetodynamics,

$$\begin{aligned} \text{Magnetic Gauss' law} &: \operatorname{div} \mathbf{B} = 0, \\ \text{Faraday's law} &: \partial_t \mathbf{B} + \operatorname{curl} \mathbf{E} = 0. \end{aligned}$$

The second Maxwell equation with source, $\delta F = J$, gives vector electrostatics and electrodynamics,

$$\begin{aligned} \text{Electric Gauss' law} &: \operatorname{div} \mathbf{E} = 4\pi\rho, \\ \text{Ampère's law} &: \partial_t \mathbf{E} - \operatorname{curl} \mathbf{B} = -4\pi\mathbf{j}. \end{aligned}$$

Maxwell's equations are generally applied to macroscopic averages of the fields, which vary wildly on a microscopic scale in the vicinity of individual atoms, where they undergo quantum effects as well (see below).

3.2 Electrodynamical action

The standard *Lagrangian* for the free electromagnetic field, $F = dA$, is given by [23, 24, 25]

$$\mathcal{L}(A) = \frac{1}{2}(F \wedge \star F),$$

and for the gauge potential

$$A_\mu \mapsto A_\mu + \frac{1}{e}(\partial_\mu \Lambda),$$

then the gauge-covariant derivative,

$$D_\mu = \partial_\mu - ieA_\mu$$

transforms as

$$D_\mu \mapsto \partial_\mu - ieA_\mu - i(\partial_\mu \Lambda)$$

and $D_\mu \psi$ transforms as

$$D_\mu \mapsto \partial_\mu - ieA_\mu - i(\partial_\mu \Lambda).$$

with the corresponding action

$$S(A) = \frac{1}{2} \int F \wedge \star F.$$

Using the Hodge L^2 -inner product (2), we can rewrite this action as

$$S(A) = \frac{1}{2}(F, F). \tag{3}$$

3.3 2D electrodynamics

One of the reasons that gauge electrodynamics in 2D is especially simple is that the electromagnetic field $F = dA$, being a 2-form, can be written simply as a scalar field $\varphi = \varphi(x, t)$ times the volume form [44]

$$F = \varphi \text{ vol}.$$

This means that the only Hodge duals we need to consider are the trivial ones,

$$\star \text{ vol} = 1 \quad \text{and} \quad \star 1 = \text{ vol},$$

so the 2D Lagrangian for vacuum electrodynamics is given by [43]

$$L = \frac{1}{2}(\varphi \text{ vol}) \wedge \star(\varphi \text{ vol}) = \frac{1}{2}\varphi^2 \text{ vol} \wedge 1 = \frac{\varphi^2}{2}\text{ vol}.$$

4 Quantum Electrodynamics in 4D

Quantum electrodynamics (QED) is a relativistic quantum field theory of electrodynamics. QED was developed by four Nobel Laureates, P. Dirac, R. Feynman, J. Schwinger and S. Tomonaga, and F. Dyson, between 1920s and 1950s. It describes some aspects of how electrons, positrons and photons interact. QED mathematically describes all phenomena involving electrically charged particles interacting by means of exchange of photons.

4.1 Dirac QED

The *Dirac equation* for a particle with mass m (in natural units) reads (see, e.g., [25])

$$(i\gamma^\mu \partial_\mu - m)\psi = 0, \quad (\mu = 0, 1, 2, 3) \tag{4}$$

where $\psi = \sqrt{-1} \psi(x)$ is a 4-component spinor²⁰ wave-function, the so-called Dirac spinor, while γ^μ are 4×4 Dirac γ -matrices,

$$\begin{aligned} \gamma^0 &= \begin{pmatrix} 1 & 0 & 0 & 0 \\ 0 & 1 & 0 & 0 \\ 0 & 0 & -1 & 0 \\ 0 & 0 & 0 & -1 \end{pmatrix}, & \gamma^1 &= \begin{pmatrix} 0 & 0 & 0 & 1 \\ 0 & 0 & 1 & 0 \\ 0 & -1 & 0 & 0 \\ -1 & 0 & 0 & 0 \end{pmatrix}, \\ \gamma^2 &= \begin{pmatrix} 0 & 0 & 0 & -i \\ 0 & 0 & i & 0 \\ 0 & i & 0 & 0 \\ -i & 0 & 0 & 0 \end{pmatrix}, & \gamma^3 &= \begin{pmatrix} 0 & 0 & 1 & 0 \\ 0 & 0 & 0 & -1 \\ -1 & 0 & 0 & 0 \\ 0 & 1 & 0 & 0 \end{pmatrix}. \end{aligned}$$

They obey the *anticommutation relations*

$$\{\gamma^\mu, \gamma^\nu\} = \gamma^\mu \gamma^\nu + \gamma^\nu \gamma^\mu = 2g^{\mu\nu},$$

where $g_{\mu\nu}$ is the metric tensor.

Dirac's γ -matrices are conventionally derived as

$$\gamma^k = \begin{pmatrix} 0 & \sigma^k \\ -\sigma^k & 0 \end{pmatrix}, \quad (k = 1, 2, 3)$$

where σ^k are *Pauli σ -matrices*²¹ (a set of 2×2 complex Hermitian and unitary matrices), defined as

$$\sigma_1 = \sigma_x = \begin{pmatrix} 0 & 1 \\ 1 & 0 \end{pmatrix}, \quad \sigma_2 = \sigma_y = \begin{pmatrix} 0 & -i \\ i & 0 \end{pmatrix}, \quad \sigma_3 = \sigma_z = \begin{pmatrix} 1 & 0 \\ 0 & -1 \end{pmatrix},$$

obeying both the commutation and anticommutation relations

$$[\sigma_i, \sigma_j] = 2i \varepsilon_{ijk} \sigma_k, \quad \{\sigma_i, \sigma_j\} = 2\delta_{ij} \cdot I,$$

where ε_{ijk} is the Levi-Civita symbol, δ_{ij} is the Kronecker delta, and I is the identity matrix.

²⁰The most convenient definitions for the 2-spinors, like the Dirac spinor, are:

$$\phi^1 = \begin{bmatrix} 1 \\ 0 \end{bmatrix}, \quad \phi^2 = \begin{bmatrix} 0 \\ 1 \end{bmatrix} \quad \text{and} \quad \chi^1 = \begin{bmatrix} 0 \\ 1 \end{bmatrix}, \quad \chi^2 = \begin{bmatrix} 1 \\ 0 \end{bmatrix}.$$

²¹In quantum mechanics, each Pauli matrix represents an observable describing the spin of a spin $\frac{1}{2}$ particle in the three spatial directions. Also, $i\sigma_j$ are the generators of rotation acting on non-relativistic particles with spin $\frac{1}{2}$. The state of the particles are represented as two-component spinors.

In *quantum information*, single-qubit quantum gates are 2×2 unitary matrices. The Pauli matrices are some of the most important single-qubit operations.

Now, the Lorentz-invariant form of the Dirac equation (4) for an electron with a charge e and mass m_e , moving with a 4-momentum 1-form $p = p_\mu dx^\mu$ in a classical electromagnetic field defined by 1-form $A = A_\mu dx^\mu$, reads (see, e.g., [39, 25]):

$$\{i\gamma^\mu [p_\mu - eA_\mu] - m_e\} \psi(x) = 0, \quad (5)$$

and is called the *covariant Dirac equation*.

The formal QED Lagrangian (density) includes three terms,

$$\mathcal{L}(x) = \mathcal{L}_{\text{em}}(x) + \mathcal{L}_{\text{int}}(x) + \mathcal{L}_{\text{e-p}}(x), \quad (6)$$

related respectively to the free electromagnetic field 2-form $F = F_{\mu\nu} dx^\mu \wedge dx^\nu$, the electron-positron field (in the presence of the external vector potential 1-form A_μ^{ext}), and the interaction field (dependent on the charge-current 1-form $J = J_\mu dx^\mu$). The free electromagnetic field Lagrangian in (6) has the standard electrodynamic form

$$\mathcal{L}_{\text{em}}(x) = -\frac{1}{4} F^{\mu\nu} F_{\mu\nu},$$

where the electromagnetic fields are expressible in terms of components of the potential 1-form

$A = A_\mu dx^\mu$ by

$$F_{\mu\nu} = \partial_\mu A_\nu^{\text{tot}} - \partial_\nu A_\mu^{\text{tot}}, \quad \text{with} \quad A_\mu^{\text{tot}} = A_\mu^{\text{ext}} + A_\mu.$$

The electron-positron field Lagrangian is given by Dirac's equation (5) as

$$\mathcal{L}_{\text{e-p}}(x) = \bar{\psi}(x) \{i\gamma^\mu [p_\mu - eA_\mu^{\text{ext}}] - m_e\} \psi(x),$$

where $\bar{\psi}(x)$ is the Dirac adjoint spinor wave function.

The interaction field Lagrangian

$$\mathcal{L}_{\text{int}}(x) = -J^\mu A_\mu,$$

accounts for the interaction between the uncoupled electrons and the radiation field.

The field equations deduced from (6) read

$$\begin{aligned} \{i\gamma^\mu [p_\mu - eA_\mu^{\text{ext}}] - m_e\} \psi(x) &= \gamma^\mu \psi(x) A_\mu, \\ \partial^\mu F_{\mu\nu} &= J_\nu. \end{aligned} \quad (7)$$

The formal QED requires the solution of the system (7) when $A^\mu(x)$, $\psi(x)$ and $\bar{\psi}(x)$ are quantized fields.

4.2 Feynman QED

In Feynman's form of quantum electrodynamics [40, 24, 25], the process of quantization is transparent – it is performed using his path integral formalism, resulting in the quantum–field transition given (in natural units) by:

$$\langle out_A A | in_A \rangle = \int \mathcal{D}[A] e^{iS(A)} \xrightarrow{Wick} \int \mathcal{D}[A] e^{-S(A)}, \quad (8)$$

with action $S(A)$ given by (13) in the exponent (multiplied by the imaginary unit i). The Lebesgue integration in (8) is performed over electromagnetic fields A_μ , with the Lebesgue measure

$$\mathcal{D}[A] = \lim_{N \rightarrow \infty} \prod_{s=1}^N dA_\mu^s \quad (\mu = 1, \dots, 4).$$

The transformation \xrightarrow{Wick} denotes the so-called Wick-rotation of the time variable t to imaginary values $t \mapsto \tau = it$, thereby transforming the complex-valued path integral into the real-valued (Euclidean) one. The absolute square of the transition amplitude (8) gives the transition probability density function, $P(A) = |\langle out_A | in_A \rangle|^2$. Full discretization of (8) ultimately gives the standard thermodynamic partition function

$$Z = \sum_j e^{-E^j/T}, \quad (9)$$

where E^j is the energy eigenvalue, T is the temperature environmental control parameter, and the sum runs over all j energy eigenstates. From (9), we can further calculate all thermodynamical and statistical properties [41], as for example, transition entropy $S = k_B \ln Z$, etc.

The standard QED considers the path integral

$$\begin{aligned} Z[A] &= \int \mathcal{D}[A] e^{iS[A]}, \quad \text{where the action for the free e.-m. field is} \\ S[A] &= \int d^4x \left[-\frac{1}{4} (F_{\mu\nu})^2 \right] = \frac{1}{2} \int d^4x A_\mu(x) (\partial^2 g^{\mu\nu} - \partial^\mu \partial^\nu) A_\nu(x). \end{aligned}$$

$Z[A]$ is the path integral over each of the four spacetime components:

$$\mathcal{D}[A] = \mathcal{D}[A]^0 \mathcal{D}[A]^1 \mathcal{D}[A]^2 \mathcal{D}[A]^3.$$

This functional integral is badly divergent, due to gauge invariance. Recall that $F_{\mu\nu}$, and hence L , is invariant under a general gauge transformation of the form

$$A_\mu(x) \rightarrow A_\mu(x) + \frac{1}{e} \partial_\mu \alpha(x).$$

The troublesome modes are those for which $A_\mu(x) = \partial_\mu \alpha(x)$, that is, those that are gauge-equivalent to $A_\mu(x) = 0$. The path integral is badly defined because we are redundantly integrating over a continuous infinity of physically equivalent field configurations. To fix this problem, we would like to isolate the interesting part of the path integral, which counts each physical configuration only once. This can be accomplished using the *Faddeev–Popov trick* [42], which effectively adds a term to the system Lagrangian and after which we get

$$Z[A] = \int \mathcal{D}[A] \exp \left[i \int_{-T}^T d^4x \left[\mathcal{L} - \frac{1}{2\xi} (\partial^\mu A_\mu)^2 \right] \right],$$

where ξ is any finite constant.

Now, the observable O in the quantum field theory is a real-valued function of the gauge field: $O: \mathcal{A} \rightarrow \mathbb{R}$, where \mathcal{A} is the space of connections, so we can try to calculate its expected value using the electrodynamic action $S(A)$ (13) as

$$\langle \Omega | T \mathcal{O}(A) | \Omega \rangle = \frac{\int_{\mathcal{A}} \mathcal{D}[A] \mathcal{O}(A) e^{-S(A)}}{\int_{\mathcal{A}} \mathcal{D}[A] e^{-S(A)}}.$$

In certain cases, it might be difficult to define exactly what this means. Even in the finite dimensional case, where $\mathcal{D}[A]$ is the Lebesgue measure on \mathcal{A} , when we try to calculate $\langle O \rangle$ by the above formula we usually run into serious problems. To see this, let us do a sample calculation of the integral in the denominator, which is the partition function

$$Z := \int_{\mathcal{A}} \mathcal{D}[A] e^{-S(A)} \tag{10}$$

against which all other expected values are normalized.

Thus, the Faddeev–Popov trick needs also to be applied to the formula for the two-point correlation function

$$\langle \Omega | T \mathcal{O}(A) | \Omega \rangle = \lim_{T \rightarrow \infty(1-i\epsilon)} \frac{\int \mathcal{D}[A] \mathcal{O}(A) \exp \left[i \int_{-T}^T d^4x \mathcal{L} \right]}{\int \mathcal{D}[A] \exp \left[i \int_{-T}^T d^4x \mathcal{L} \right]},$$

which after Faddeev–Popov procedure becomes

$$\langle \Omega | T \mathcal{O}(A) | \Omega \rangle = \lim_{T \rightarrow \infty(1-i\epsilon)} \frac{\int \mathcal{D}[A] \mathcal{O}(A) \exp \left[i \int_{-T}^T d^4x \left[\mathcal{L} - \frac{1}{2\xi} (\partial^\mu A_\mu)^2 \right] \right]}{\int \mathcal{D}[A] \exp \left[i \int_{-T}^T d^4x \left[\mathcal{L} - \frac{1}{2\xi} (\partial^\mu A_\mu)^2 \right] \right]}.$$

The space of gauge transformations, \mathcal{G} , is a group which acts on the space \mathcal{A} of connections by

$$\mathcal{G} \times \mathcal{A} \rightarrow \mathcal{A}, \quad (\phi, A) \mapsto A + d\phi.$$

A common way of eliminating divergences caused by gauge freedom is gauge fixing [43], which means choosing some method to pick one representative of each gauge-equivalence class $[A]$ and doing path integrals over these. There are problems with this approach, however. In a general gauge theory, it might not even be possible to fix a smooth, global gauge over which to integrate. But even when we can do this, the arbitrary choice involved in fixing a gauge is undesirable, philosophically. Gauge fixing amounts to pretending a quotient space of \mathcal{A} , the space of connections modulo gauge transformations, is a subspace. A better approach is to use the quotient space directly. Namely, modding out by the action of \mathcal{G} on \mathcal{A} gives the quotient space \mathcal{A}/\mathcal{G} consisting of gauge-equivalence classes of connections, and we do path integrals like

$$Z = \int_{\mathcal{A}/\mathcal{G}} d[A] e^{-S([A])}.$$

When gauge fixing works, path integrals over \mathcal{A}/\mathcal{G} give the same results as gauge fixing. But integrating over \mathcal{A}/\mathcal{G} is more general and involves no arbitrary choices.

Since gauge equivalent connections are regarded as physically equivalent, the quotient space \mathcal{A}/\mathcal{G} of connections mod gauge transformations is sometimes called the physical configuration space for vacuum electrodynamics. A physical observable is then any real-valued function on the physical configuration space, $O : \mathcal{A}/\mathcal{G} \rightarrow \mathbb{R}$, or equivalently, any gauge-invariant function on the space \mathcal{A} of connections. In the case of noncompact gauge group even factoring out all of the gauge freedom may be insufficient to regularize our path integrals. In particular, there are certain topological conditions our space-time must meet for this programme to give convergent path integrals. As a consequence, in the case where the gauge group is \mathbb{R} , we must sometimes take more drastic measures in order to extract meaningful results, and this leads to some interesting differences between the cases $G = \mathbb{R}$ and $G = U(1)$ as the gauge group for electrodynamics. These differences are related to the famous ‘Bohm–Aharonov effect’ [43].

4.3 Cohomology criterion for path-integral convergence

To eliminate the divergences in the path integral (10) it is necessary that we eliminate any gauge freedom from the space of connections \mathcal{A} . In gauge theory, the action $S(A)$ is invariant under the group of gauge transformations \mathcal{G} . In case of a gauge group $\mathcal{G} = \mathbb{R}$, we have gauge transformations of the form

$$A \mapsto A + d\varphi,$$

where φ is an arbitrary $(p-1)$ -cochain. In other words, two p -connections are gauge equivalent if they differ by a p -coboundary $d\varphi \in B^p$. Before we saw that the existence of gauge freedom implied path integrals such as the one above must diverge [43]. The

standard procedure of eliminating any gauge freedom from the space of connections \mathcal{A} is to pass to the quotient space

$$\mathcal{A}/\mathcal{G} = C^p/B^p,$$

that is, p -connections modulo gauge transformations, effectively declaring gauge equivalent p -connections to be equal. In particular, the criterion in \mathbb{R} electrodynamics for path integrals over the physical configuration space \mathcal{A}/\mathcal{G} to converge is that the first cohomology be trivial [43]:

$$\left(\begin{array}{c} Z = \int_{\mathcal{A}/\mathcal{G}} \mathcal{D}[A] e^{-S(A)} \\ \text{converges for } \mathbb{R} \text{ electrodynamics} \end{array} \right) \iff H^1 = 0.$$

5 Electro–Muscular Stimulation

In this section we develop covariant biophysics of electro–muscular stimulation, as an externally induced generator of the *covariant muscular force*,

$$F_i = m_{ij} a^j, \tag{11}$$

where F_i are covariant components of the muscular force (torque) 1–form $F = F_i(t) dx^i$, m_{ij} are the covariant components of the musculo-skeletal metric/inertia tensor $m = m_{ij} dx^i \otimes dx^j$, while $a^i = a^i(t) \partial_{x^i}$ are contravariant components of the angular acceleration vector (see [22, 23] for technical details). The so-called *functional electrical stimulation* (FES) of human skeletal muscles is used in rehabilitation and in medical orthotics to externally stimulate the muscles with damaged neural control. However, the repetitive use of electro–muscular stimulation, besides functional, causes also structural changes in the stimulated muscles, giving the physiological effect of muscular training.

The use of low and very low frequency impulses in the body, delivered through electrodes, is known as transcutaneous stimulation of the nerves, electro–acupuncture and electro–stimulation. Here, an electromagnetic field accompanies the passage of the electric current through the conductive wire. This is generally known as the term ‘electromagnetic therapy’.²²

²²In the original sense acupuncture meant the inserting of needles in specific regions of the body. Electro–acupuncture supplies the body with low–volt impulses through the medium of surface electrodes to specific body regions or by non specific electrodes. Transcutaneous electric stimulation of the nerves (TENS) has for years been a well known procedure in conventional medicine. The impulses that are produced with this type of stimulation, are almost identical with those of electro–stimulation, yet many doctors still assume, that they are two different therapies. This has resulted in TENS being considered as a daily therapy, while electro–acupuncture or electro–stimulation were treated as ‘alternative therapy’. Apart from the fact, that electro–acupuncture electro–impulses are delivered through needles, both therapies should be considered identical. Patients, who have reservations about the use of needles, can by the use of electric impulses

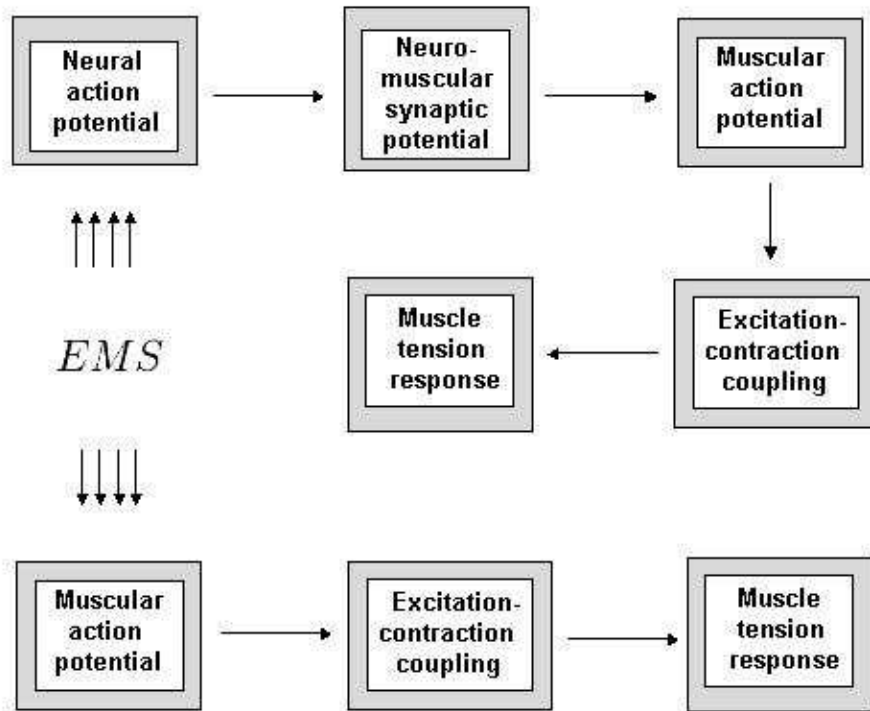


Figure 4: Schematic of electro-muscular stimulation (*EMS*).

In particular, *electro-muscular stimulation* (*EMS*, see Figure 4) represents a union of external electrical stimulation fields, internal myofibrillar excitation-contraction paths,

over surface electrodes on the skin, have a satisfactory alternative (see Figure 4). We choose the term electro-stimulation, because the acupuncture system is not included in all therapies. Clinical tests have showed that there are two specific types of reactions:

- The first reaction is spontaneous and dependent on the choice of body region. The stimulation of this part of the body results in an unloading, that can be compared with that of a battery. Normally this goes hand in hand with an immediate improvement in the patient. This effect of unloading may also be reached by non-specific electric stimulation.
- The second normal reaction is of a delayed nature, that results in relaxation and control of pain. Moreover two other important effects follow, that begin between 10 and 20 minutes after the start of the treatment. This reaction is associated (combined) with different chemicals, such as beta-endorphins and 5-hydroxytryptamins. When using low and very low frequency stimulations, the second effect is obtained by the utilization of specific frequencies on the body. This is independent of the choice of a specific part of the body, because the connected electromagnet makes the induction of secondary electric current in the whole body possible.

and dissipative skin & fat geometries, formally given by

$$EMS = EMS_{fields} \cup EMS_{paths} \cup EMS_{geom}. \quad (12)$$

In Feynman's QED formulation, corresponding to each of the three *EMS*-phases in (12) we formulate:

1. The *least action principle*, to model a unique, external-anatomical, predictive and smooth, macroscopic *EMS* field-path-geometry; and
2. Associated *Feynman path integral*, to model an ensemble of rapidly and stochastically fluctuating, internal, microscopic, fields-paths-geometries of the cellular *EMS*, to which the external-anatomical macro-level represents both time and ensemble *average*.²³

In the proposed formalism, muscular excitation-contraction paths $x^i(t)$ are caused by electromagnetic stimulation fields $\Phi^k = \Phi^k(t, x, y, z)$, by the the Lorenz force equation (1), while they are both affected by dissipative and noisy skin & fat shapes and curvatures, defined by the local Riemannian musculo-skeletal metric tensor m_{ij} (11). In particular, the electromagnetic 2-form Faraday $F = F_{\alpha\beta} dx_\alpha dx_\beta$, defines the Lorentz force 1-form $Q = Q_\alpha dx_\alpha$ of the electro-muscular stimulation,

$$Q_\alpha \equiv \dot{p}_\alpha \propto q F_{\alpha\beta} v^\beta,$$

where q is total electric charge and v^β is the velocity vector-field of the stimulation flow. This equation says that the muscular force 1-form Q_α generated by the simulation is proportional to the stimulation field strength $F_{\alpha\beta}$, velocity of the stimulation flow v^β through the skin-fat-muscle tissue, as well as the total stimulation charge q .

In the following text, we first formulate the global model for the *EMS*, to set up the general formalism to be specialized subsequently for each of the three *EMS*-phases.

5.1 Global macro *EMS*-level

In general, at the *macroscopic EMS*-level we first formulate the *total action* $S[\Phi]$, our central quantity, which can be described through physical dimensions of *Energy* \times *Time* = *Effort*, which is also the dimension of the *Planck constant* \hbar (= 1 in normal units). This total action quantity has immediate biophysical ramifications: *the greater the action – the higher the stimulation effect on the new shape*. The action $S[\Phi]$ depends on macroscopic fields, paths and geometries, commonly denoted by an abstract field symbol Φ^i . The

²³Recall that *ergodic hypothesis* equates *time average* with *ensemble average*.

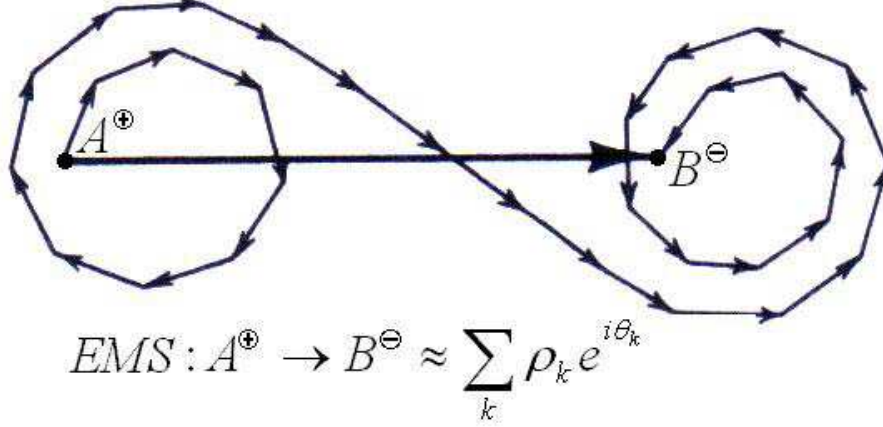


Figure 5: Simplified Feynman-like experimental approach to electrical muscular stimulation: the flow of electric current from the positive surface pad A^\oplus to the negative pad B^\ominus can be approximated by the vector sum of complex vectors $\rho_k e^{i\theta_k}$, where θ_k are proportional to the time taken by each vector ρ_k ; this vector sum will be further developed into Feynman integral.

action $S[\Phi]$ is formally defined as a temporal integral from the *initial* time instant t_{ini} to the *final* time instant t_{fin} ,

$$S[\Phi] = \int_{t_{ini}}^{t_{fin}} \mathfrak{L}[\Phi] dt, \quad (13)$$

with *Lagrangian density*, given by

$$\mathfrak{L}[\Phi] = \int d^n x \mathcal{L}(\Phi^i, \partial_{x^j} \Phi^i),$$

where the integral is taken over all n coordinates $x^j = x^j(t)$ of the *EMS*, and $\partial_{x^j} \Phi^i$ are time and space partial derivatives of the Φ^i -variables over coordinates.

Second, we formulate the *least action principle* as a minimal variation δ of the action $S[\Phi]$

$$\delta S[\Phi] = 0, \quad (14)$$

which, using variational *Euler-Lagrangian equations*, derives field-motion-geometry of the unique and smooth *EMS*-transition map (or, more appropriately, ‘functor’ [24])

$$\mathcal{T} : STIMUL_{t_{ini}} \Rightarrow CONTRACT_{t_{mid}} \Rightarrow SHAPE_{t_{fin}},$$

acting at a macro-level from some initial time t_{ini} to the final time t_{fin} (via the intermediate time t_{mid}).²⁴

In this way, we get macro-objects in the global *EMS*: a single electrodynamic stimulation field described by Maxwell field equations, a single muscular excitation-contraction path described by Lagrangian equation of motion, and a single Riemannian skin & fat geometry.

5.2 Local Micro *EMS*-level

After having properly defined macro-level *EMS*, we move down to the *microscopic cellular EMS*-level of rapidly fluctuating electrodynamic fields, sarcomere-contraction paths and coarse-grained, fractal muscle-fat geometry, where we cannot define a unique and smooth field-path-geometry. The most we can do at this level of *fluctuating noisy uncertainty*, is to formulate an adaptive path integral and calculate overall probability amplitudes for ensembles of local transitions from negative *EMS*-pad A^\ominus to the positive pad B^\oplus (see Figure 5). This *probabilistic transition micro-dynamics* is given by a multi field-path-geometry, defining the microscopic *transition amplitude* corresponding to the macroscopic *EMS*-transition map \mathcal{T} . So, what is externally the transition map, internally is the transition amplitude. The absolute square of the transition amplitude is the *transition probability*.

Now, the total *EMS*-transition amplitude, from the initial state *STIMUL*, to the final state *SHAPE*, is defined on *EMS*

$$\langle SHAPE | STIMUL \rangle : STIMUL_{t_0} \Rightarrow SHAPE_{t_1}, \quad (15)$$

given by *modern adaptive generalization* of the Feynman's path integral, see [25]). The transition map (15) calculates *overall probability amplitude* along a multitude of wildly fluctuating fields, paths and geometries, performing the *microscopic* transition from the micro-state $STIMUL_{t_0}$ occurring at initial micro-time instant t_0 to the micro-state $SHAPE_{t_1}$ at some later micro-time instant t_1 , such that all micro-time instants fit inside the global

²⁴Here, we have in place *n-categorical Lagrangian-field structure* on the *muscular Riemannian configuration manifold M* [24]

$$\Phi^i : [0, 1] \rightarrow M, \Phi^i : \Phi_0^i \mapsto \Phi_1^i,$$

using

$$\frac{d}{dt} f_{\dot{x}^i} = f_{x^i} \Rightarrow \partial_\mu \left(\frac{\partial \mathcal{L}}{\partial_\mu \Phi^i} \right) = \frac{\partial \mathcal{L}}{\partial \Phi^i},$$

with

$$[x_0, x_1] \mapsto [\Phi_0^i, \Phi_1^i].$$

transition interval $t_0, t_1, \dots, t_s \in [t_{ini}, t_{fin}]$. It is symbolically written as

$$\langle SHAPE | STIMUL \rangle = \int \mathcal{D}[w\Phi] e^{iS[\Phi]}, \quad (16)$$

where the Lebesgue integration is performed over all continuous $\Phi_{con}^i = fields + paths + geometries$, while summation is performed over all discrete processes and regional topologies Φ_{dis}^j . The symbolic differential $\mathcal{D}[w\Phi]$ in the general path integral (16), represents an *adaptive path measure*, defined as a weighted product

$$\mathcal{D}[w\Phi] = \lim_{N \rightarrow \infty} \prod_{s=1}^N w_s d\Phi_s^i, \quad (i = 1, \dots, n = con + dis), \quad (17)$$

which is in practice satisfied with a large N .

In this way, we get a range of micro-objects in the local *EMS* at the short time-level: ensembles of rapidly fluctuating, noisy and crossing electrical stimulation fields, myofibrillar contraction paths and local skin & fat shape-geometries. However, by averaging process, both in time and along ensembles of fields, paths and geometries, we can recover the corresponding global, smooth and fully predictive, external *EMS* transition-dynamics \mathcal{T} .

5.3 Micro-Level Adaptation and Muscular Training

The adaptive path integral (16–17) incorporates the local muscular training process according to the basic learning formula

$$NEW\ VALUE = OLD\ VALUE + INNOVATION,$$

where the term *VALUE* represents respectively *biological images* of the *STIMUL*, *CONTRACT* and *SHAPE*.

The general *synaptic weights* $w_s = w_s(t)$ in (17) are updated by the *homeostatic neuro-muscular feedbacks* during the transition process \mathcal{T} , according to one of the two standard neural training schemes, in which the micro-time level is traversed in discrete steps, i.e., if $t = t_0, t_1, \dots, t_s$ then $t + 1 = t_1, t_2, \dots, t_{s+1}$:

1. A *self-organized, unsupervised*, e.g., Hebbian-like training rule (see, e.g. [28]):

$$w_s(t + 1) = w_s(t) + \frac{\sigma}{\eta} (w_s^d(t) - w_s^a(t)), \quad (18)$$

where $\sigma = \sigma(t)$, $\eta = \eta(t)$ denote *signal* and *noise*, respectively, while superscripts *d* and *a* denote *desired* and *achieved* muscular micro-states, respectively; or

2. A certain form of a *supervised gradient descent training*:

$$w_s(t+1) = w_s(t) - \eta \nabla J(t), \quad (19)$$

where η is a small constant, called the *step size*, or the *training rate*, and $\nabla J(n)$ denotes the gradient of the ‘performance hyper-surface’ at the t -th iteration.

For more details EMS-fields, paths and geometries, see [25].

6 Appendix: Manifolds and Bundles

6.1 Manifolds

Smooth manifold is a curved n D space which is locally equivalent to \mathbb{R}^n . To sketch its formal definition, consider a set M (see Figure 6) which is a *candidate* for a manifold. Any point $x \in M$ ²⁵ has its *Euclidean chart*, given by a 1-1 and *onto* map $\varphi_i : M \rightarrow \mathbb{R}^n$, with its *Euclidean image* $V_i = \varphi_i(U_i)$. More precisely, a chart φ_i is defined by

$$\varphi_i : M \supset U_i \ni x \mapsto \varphi_i(x) \in V_i \subset \mathbb{R}^n,$$

where $U_i \subset M$ and $V_i \subset \mathbb{R}^n$ are open sets.

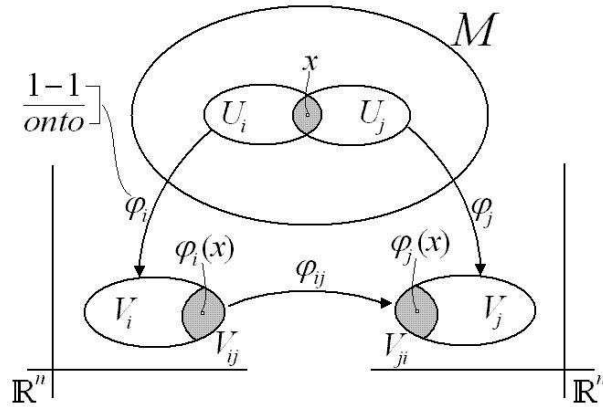


Figure 6: Geometric picture of the manifold concept.

Clearly, any point $x \in M$ can have several different charts (see Figure 6). Consider a case of two charts, $\varphi_i, \varphi_j : M \rightarrow \mathbb{R}^n$, having in their images two open sets, $V_{ij} = \varphi_i(U_i \cap U_j)$ and $V_{ji} = \varphi_j(U_i \cap U_j)$. Then we have *transition functions* φ_{ij} between them,

$$\varphi_{ij} = \varphi_j \circ \varphi_i^{-1} : V_{ij} \rightarrow V_{ji}, \quad \text{locally given by} \quad \varphi_{ij}(x) = \varphi_j(\varphi_i^{-1}(x)).$$

²⁵Note that sometimes we will denote the point in a manifold M by m , and sometimes by x (thus implicitly assuming the existence of coordinates $x = (x^i)$).

If transition functions φ_{ij} exist, then we say that two charts, φ_i and φ_j are *compatible*. Transition functions represent a general (nonlinear) *transformations of coordinates*, which are the core of classical *tensor calculus*.

A set of compatible charts $\varphi_i : M \rightarrow \mathbb{R}^n$, such that each point $x \in M$ has its Euclidean image in at least one chart, is called an *atlas*. Two atlases are *equivalent* iff all their charts are compatible (i.e., transition functions exist between them), so their union is also an atlas. A *manifold structure* is a class of equivalent atlases.

Finally, as charts $\varphi_i : M \rightarrow \mathbb{R}^n$ were supposed to be 1-1 and onto maps, they can be either *homeomorphisms*, in which case we have a *topological* (C^0) manifold, or *diffeomorphisms*, in which case we have a *smooth* (C^k) manifold.

6.2 Fibre Bundles

On the other hand, the well-known tangent bundle TM and cotangent bundle T^*M of a smooth manifold M , respectively endowed with Riemannian geometry (suitable for Lagrangian dynamics) and symplectic geometry (suitable for Hamiltonian dynamics) – are special cases of a more general geometrical object called *fibre bundle*. Here the word *fiber* V of a map $\pi : Y \rightarrow X$ denotes the *preimage* $\pi^{-1}(x)$ of an element $x \in X$. It is a space which *locally* looks like a product of two spaces (similarly as a manifold locally looks like Euclidean space), but may possess a different *global* structure. To get a visual intuition behind this fundamental geometrical concept, we can say that a fibre bundle Y is a *homeomorphic generalization* of a *product space* $X \times V$ (see Figure 7), where X and V are called the *base* and the *fibre*, respectively. $\pi : Y \rightarrow X$ is called the *projection*, $Y_x = \pi^{-1}(x)$ denotes a fibre over a point x of the base X , while the map $f = \pi^{-1} : X \rightarrow Y$ defines the *cross-section*, producing the *graph* $(x, f(x))$ in the bundle Y (e.g., in case of a tangent bundle, $f = \dot{x}$ represents a velocity vector-field, so that the graph in the bundle Y reads (x, \dot{x})).

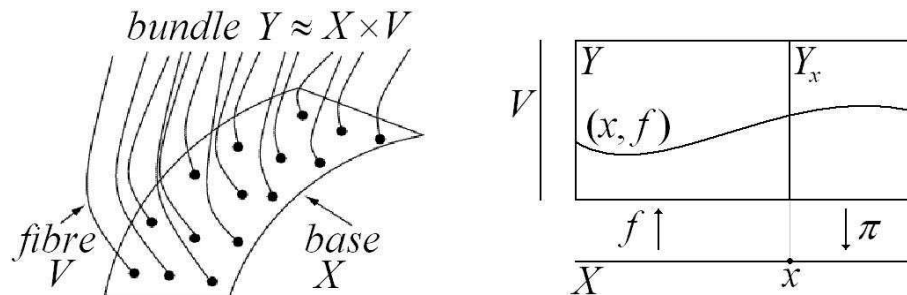


Figure 7: A sketch of a fibre bundle $Y \approx X \times V$ as a generalization of a product space $X \times V$; left – main components; right – a few details (see text for explanation).

The main reason why we need to study fibre bundles is that *all dynamical objects* (including vectors, tensors, differential forms and gauge potentials) are their *cross-sections*, representing *generalizations of graphs of continuous functions*.

References

- [1] Brazier, M.A.B. A History of the Electrical Activity of the Brain. Pitman, London, (1961).
- [2] Hodgkin, A.L., Huxley, A.F., Katz, B. Measurements of current-voltage relations in the membrane of the giant axon of Loligo. J. Physiol. 116: 424448, (1952).
- [3] Hodgkin, A.L., Huxley, A.F. Currents carried by sodium and potassium ions through the membrane of the giant axon of Loligo. J. Physiol. 116:449472, (1952).
- [4] Hodgkin, A.L., Huxley, A.F. The components of membrane conductance in the giant axon of Loligo. J. Physiol. 116:473496, (1952).
- [5] Hodgkin, A.L., Huxley, A.F. The dual effect of membrane potential on sodium conductance in the giant axon of Loligo. J. Physiol. 116: 497506, (1952).
- [6] Hodgkin, A.L., Huxley, A.F. A quantitative description of membrane current and its application to conduction and excitation in nerve. J. Physiol. 117: 500544, (1952).
- [7] Rall, W. Cable Theory for Dendritic Neurons, in C. Koch and I. Segev: Methods in Neuronal Modeling: From Synapses to Networks. Cambridge MA: Bradford Books, MIT Press, pp. 962, (1989).
- [8] Hodgkin, A.L., Rushton, W.A.H. The electrical constants of a crustacean nerve fibre. Proc. Roy. Soc. B 133: 44479, (1946).
- [9] Noble, D. Cardiac action and pacemaker potentials based on the Hodgkin-Huxley equations. Nature 188: 495497, (1960).
- [10] Kléber, A.G., Rudy, Y. Basic mechanisms of cardiac impulse propagation and associated arrhythmias. Physiol. Rev. 84 (2): 43188, (2004).
- [11] Epstein, C.M. Introduction to EEG and evoked potentials. J.B. Lippincot Co. (1983).
- [12] Braunwald, E. (ed), Heart Disease: A Textbook of Cardiovascular Medicine, (5th ed), Saunders, Philadelphia, (1997).
- [13] Mark, J.B. Atlas of cardiovascular monitoring. Churchill Livingstone, New York, (1998).

- [14] Cram, J.R., Kasman, G.S., Holtz, J., Introduction to Surface Electromyography. Aspen Publishers Inc., Gaithersburg, Maryland, (1998).
- [15] Reaz, M.B.I., Hussain, M.S., Mohd-Yasin, F., Techniques of EMG Signal Analysis: Detection, Processing, Classification and Applications, Biological Procedures Online, vol. 8, issue 1, pp. 11-35, (2006).
- [16] D.O. Carpenter, S. Ayrapetyan, Biological Effects of Electric and Magnetic Fields, (Volumes 1 & 2), Academic Press, New York, (1994).
- [17] E. Valentini, G. Curcio, F. Moroni, M. Ferrara, L. De Gennaro, M. Bertini, Neurophysiological Effects of Mobile Phone Electromagnetic Fields on Humans: A Comprehensive Review, Bioelectromagnetics 28:415432, (2007).
- [18] J.M. Elwood, Epidemiological Studies of Radio Frequency Exposures and Human Cancer, Bioelectromagnetics Supplement 6:S63S73, (2003).
- [19] G. Vincze, A. Szasz, A.R. Liboff, New Theoretical Treatment of Ion Resonance Phenomena, Bioelectromagnetics 29:380386, (2008).
- [20] J.E. Marsden, A. Tromba, Vector Calculus (5th ed.), W. Freeman and Company, New York, (2003)
- [21] V. Ivancevic, Symplectic Rotational Geometry in Human Biomechanics, SIAM Rev. 46, 3, 455–474, (2004).
- [22] V. Ivancevic, T. Ivancevic, Human–Like Biomechanics. Springer, Dordrecht, (2006).
- [23] V. Ivancevic, T. Ivancevic, Geometrical Dynamics of Complex Systems. Springer, Dordrecht, (2006).
- [24] V. Ivancevic, T. Ivancevic, Applied Differential Geometry: A Modern Introduction. World Scientific, Singapore, (2007)
- [25] V. Ivancevic, T. Ivancevic, Quantum Leap: From Dirac and Feynman, Across the Universe, to Human Body and Mind. World Scientific, Singapore, (2008)
- [26] V. Ivancevic, T. Ivancevic, High–Dimensional Chaotic and Attractor Systems. Springer, Berlin, (2006).
- [27] V. Ivancevic, T. Ivancevic, Natural Biodynamics. World Scientific, Singapore, (2006)
- [28] V. Ivancevic, T. Ivancevic, Neuro-Fuzzy Associative Machinery for Comprehensive Brain and Cognition Modelling. Springer, Berlin, (2007)

- [29] V. Ivancevic, T. Ivancevic, Computational Mind: A Complex Dynamics Perspective. Springer, Berlin, (2007)
- [30] Abraham, R., Marsden, J., Ratiu, T., Manifolds, Tensor Analysis and Applications. Springer, New York, (1988).
- [31] Choquet-Bruhat, Y., DeWitt-Morete, C., Analysis, Manifolds and Physics (2nd ed). North-Holland, Amsterdam, (1982).
- [32] Voisin, C., Hodge Theory and Complex Algebraic Geometry I. Cambridge Univ. Press, Cambridge, (2002).
- [33] De Rham, G., Differentiable Manifolds. Springer, Berlin, (1984).
- [34] Flanders, H., Differential Forms: with Applications to the Physical Sciences. Acad. Press, (1963).
- [35] C.W. Misner, K.S. Thorne, J.A. Wheeler, Gravitation. W. Freeman and Company, New York, (1973).
- [36] I. Ciufolini, J.A. Wheeler, Gravitation and Inertia, Princeton Series in Physics, Princeton University Press, Princeton, New Jersey, (1995).
- [37] P.H. Frampton, Gauge Field Theories, Frontiers in Physics. Addison-Wesley, (1986).
- [38] J.C. Baez, J.P. Muniain, Gauge Fields, Knots and Gravity, Series on Knots and Everything – Vol. 4. World Scientific, Singapore, (1994).
- [39] Drake, G.W.F (ed.), Springer Handbook of Atomic, Molecular, and Optical Physics. Springer, New York, (2006)
- [40] R.P. Feynman, Quantum Electrodynamics. Advanced Book Classics, Perseus Publishing, (1998).
- [41] R.P. Feynman, Statistical Mechanics, A Set of Lectures. WA Benjamin, Inc., Reading, Massachusetts, (1972).
- [42] L.D. Faddeev and V.N. Popov, Feynman diagrams for the Yang–Mills field. Phys. Lett. B **25**, 29, (1967).
- [43] D.K. Wise, p-form electrodynamics on discrete spacetimes. Class. Quantum Grav. **23**, 5129–5176, (2006).
- [44] E. Witten, On quantum gauge theories in two dimensions, Commun. Math. Phys. **141**, 153–209, (1991).